An Optimization-based Time-optimal Velocity Planning for Autonomous Driving

Hao HU, Weigang PAN, Song GAO*, Xiangmeng TANG

School of Information Science and Electrical Engineering, Shangdong Jiaotong University,
5001 Haitang Road, Jinan, 250000, Shandong, China
huhao199709@163.com, panweigang1980@163.com,
gaosong@sdjtu.edu.cn (**Corresponding author*), tang_xm@hrbeu.edu.cn

Abstract: Velocity planning plays an important role in motion planning of automated driving as it must meet safety, comfort, and traffic regulation requirements. Therefore, it is necessary to consider Jerk constraint and dynamic obstacle constraint. However, the introduction of these constraints makes velocity planning a non-convex optimization problem, significantly increasing computational complexity. To address these challenges, this paper investigates an optimization-based time-optimal velocity planning method. The non-convex and non-linear problems caused by Jerk constraint and dynamic obstacle constraint are addressed by realizing constraint linearization through velocity filtering with acceleration as the threshold. The linear programming (LP) method is then used twice to calculate a time-optimal velocity profile that satisfies the given constraints. Furthermore, when hard constraints are unable to satisfy obstacle avoidance planning, a dynamic constraint frame strategy is proposed to relax the hard constraints and fully utilize the dynamic performance of the ego-vehicle to avoid obstacles. Finally, simulations are conducted in various driving scenarios to validate the effectiveness of the proposed approach. The simulation results demonstrate that the approach proposed in this paper can quickly generate velocity profiles that meet safety and comfort constraints, within a short planning period. Additionally, the dynamic constraint frame strategy can improve the dynamic adaptability of the algorithm.

Keywords: Autonomous driving, Motion planning, Jerk limitation, Velocity planning, Vehicle safety.

1. Introduction

Over the past few decades, with the rapid development of autonomous driving algorithms, research has expanded from the ability to safely reach a designated destination to incorporating constraints such as comfort into motion planning (Li et al., 2022). In the application of autonomous driving technology, velocity planning played a vital role, with significant implications for efficiency, safety, comfort, and various other factors (Subotić et al., 2022). Concerning safety, velocity planning is essential, whether for changing lanes to overtake, braking to follow, or stopping to avoid obstacles. Especially when there is no space to adjust the path choice to avoid a collision, it is a more sensible decision to achieve obstacle avoidance by adjusting velocity (Jian et al., 2022). Regarding comfort, when autonomous driving vehicles need to avoid obstacles during commuting or travelling, such as in continuous traffic light sections, velocity planning without comfort constraints can result in a terrible ride experience for passengers and may even cause motion sickness (Jones et al., 2019). Therefore, a good velocity planning is crucial in ensuring both driving safety and meeting the comfort needs of passengers.

By analyzing the problems associated with autonomous driving in urban driving scenarios, three core metrics for velocity planning algorithms have been summarized in this paper: simultaneity, safety and comfort.

High simultaneity performance was required for velocity planning algorithms to plan optimal trajectories quickly, in complex environmental scenarios (Chen et al., 2019; Yang et al., 2022). Continuous optimization algorithms have gained attention in recent years for their ability to define cost functions and constraint equations almost simultaneously (Consolini et al., 2017; Consolini et al., 2022). These approaches transform velocity planning into minimum time or minimum Jerk problems, which can be efficiently solved using optimization algorithms. Various solutions had been proposed by researchers for the minimum time velocity planning problem. Wang, Liu & Zheng (2021) utilized optimization algorithms to find the time-optimal velocity profile satisfying vehicle dynamics constraints in terms of lateral and longitudinal acceleration. The approach proposed in (Cabassi, Consolini & Locatelli, 2018) performed three iterations to achieve the optimal solution for minimum time optimal velocity planning on a given path, which reduced computational and logical operations.

Optimization algorithms have been widely used in velocity planning due to their high real-time performance. Most papers that employed optimization algorithms set hard constraints, such as acceleration and Jerk, which often caused planner solution failures in unknown and complex scenarios (Guarino Lo Bianco,

https://doi.org/10.24846/v32i3y202304 ICI Bucharest © Copyright 2012-2023. All rights reserved

2013; Ni et al., 2022). Setting the constraint value too low reduced the algorithm solution space and limited the exploitation of vehicle dynamic performance. On the other hand, if the constraint was set too high, passenger comfort would be compromised. To address the issue of hard constraints lacking dynamic adaptability, researchers applied punishment to soften the constraints as in (Zhang et al., 2018). In (Artuñedo, Villagra & Godoy, 2021), a fallback strategy was proposed to generate an obstacle avoidance velocity profile by providing larger constraint values, when the constraints failed to provide a solution for the planner. However, this algorithm has low efficiency under its fallback strategy. Therefore, a method was needed to not only guarantee the real-time performance of the algorithm but also improve its dynamic adaptation to the environment.

Velocity planning was a major way to improving comfort levels in motion planning. Experiments in (Jones et al., 2019; Mata-Carballeira, del Campo & Asua, 2021) showed that high acceleration, deceleration, and Jerk constraint were the main factors causing passenger discomfort. The introducing of acceleration and deceleration constraints in (Consolini et al., 2022) improved the comfort index. Further research in (Artuñedo, Villagra & Godoy, 2021) revealed that Jerk constraint had a greater impact on comfort levels than acceleration and deceleration through numerous experiments. However, the Jerk constraint had non-convex and non-linear characteristics, which weakened the simultaneity performance of the algorithm. To address this issue, researchers Zhang et al. (2018) used an approach called Pseudo-Jerk to simplify and linearize the Jerk constraint. However, Pseudo-Jerk deviated too much from the true value. In (Shimizu, Horibe & Watanabe, 2022), a predicted maximum velocity profile was obtained by using the maximum acceleration and Jerk constraint for the forward-backward Jerk filtering method, which in its turn linearized the Jerk constraint.

To improve the safety and comfort of autonomous driving velocity planning, this work has made three main contributions:

- An efficient simultaneous velocity linear programming solution method is proposed to solve the time-optimal velocity profile on the path quickly;
- Through a dynamic constraint frame strategy, a softened relaxation of the hard constraint is proposed to solve the maneuverability degradation of the car caused by the hard constraint of velocity planning, in the obstacle avoidance scenario, thus addressing the lack of adaptability of hard constraints in dynamic scenarios;
- The acceleration and safety avoidance model is used for obstacle velocity limitation filtering, and the linearization of Jerk constraint is achieved by using the LP method twice, in order to obtain the time-optimal velocity profile of the trajectory, aiming at addressing the non-convex and non-linear problem caused by the Jerk constraint.

This paper is organized into 6 sections. Section 2 addresses the challenge of defining velocity planning along a predetermined path, taking various constraints into account. Section 3 elaborates on the dynamic constraint framework, while Section 4 details the linearization treatment of these constraints. The effectiveness of this approach is validated through multiple simulation scenarios, as presented in Section 5. Section 6 provides concluding remarks.

2. Problem Statement

In essence, motion planning is a three-dimensional process including space and time (Perri, Guarino & Locatelli, 2015; Iancu et al., 2022). A common hierarchical motion planning framework is presented in (Fan et al., 2018) as illustrated in Figure 1.

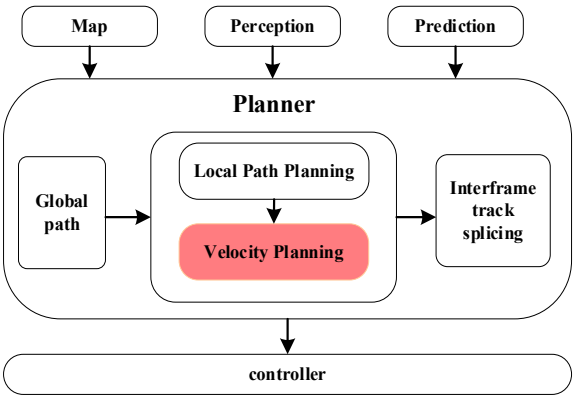

Figure 1. Layered motion planning framework

The purpose of velocity planning is to find time-saving and comfortable velocity profiles for autonomous driving that satisfy a series of constraints while ensuring driving safety.

The following passage presents the formal definition of the arc length parametric velocity planning problem. Let the arc length along the path s to be a function of time t, i.e. $s = s(t)$. The ego-vehicle travels along path s. The single-track vehicle model, depicted in Figure 2, is used to represent the actual vehicle kinematics and dynamics.

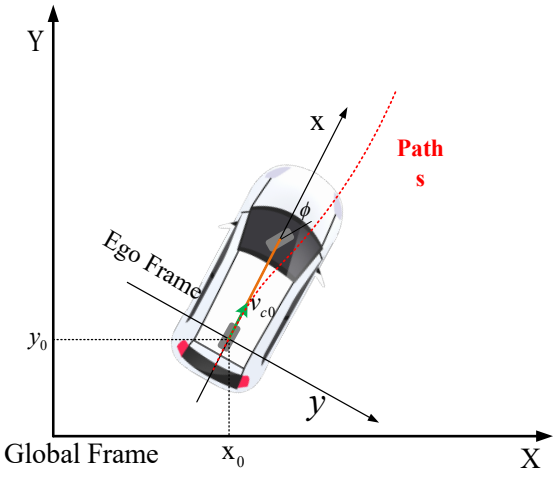

Figure 2. Vehicle kinematic models

In this paper, the decision variables for velocity planning are defined as follows:

$$\begin{cases} \beta(s) := \dot{s}^2 \\ \alpha(s) := \ddot{s} \end{cases}, \tag{1}$$

where β represents the square of the first-order derivative of path s with respect to time t and α indicates the second-order derivative of path s with respect to time t. The relationship between β and α can be obtained below:

$$\frac{d\beta}{ds} = \frac{d(\dot{s}^2)}{ds} = 2\dot{s}\frac{d\dot{s}}{ds} = 2\frac{ds}{dt}\frac{d\dot{s}}{ds} = 2\ddot{s} = 2\alpha, \tag{2}$$

where $j(s)$ is an expression for Jerk constraint along path s, defined as the first-order derivative of acceleration α with respect to time t:

$$j(s) := \dddot{s} = \dot{\alpha} = \frac{d\alpha}{dt} = \frac{d\alpha}{ds}\frac{ds}{dt} = \frac{d\alpha}{ds}\sqrt{\beta}. \tag{3}$$

When performing velocity planning, avoiding dynamic or static obstacles form the path is essential. This paper accomplishes the obstacle avoidance task by imposing a time constraint on the ego-vehicle reaching the obstacle. The arrival time T corresponding to the path s can be written as:

$$T(s) = \int_0^s \beta(l)^{-\frac{1}{2}} dl. \tag{4}$$

A normal acceleration constraint is introduced into velocity planning to prevent the vehicle from sliding sideways during driving, based on the research work from (Consolini et al., 2017). According to the acceleration constraint, maximum velocity v_{max} and curvature κ of the ego-vehicle should satisfy:

$$v_{max} \le \sqrt{\frac{\alpha_{max}^N}{\kappa}}, \tag{5}$$

The algorithm aims to plan a time-optimal velocity profile that satisfies velocity, acceleration, Jerk, and obstacle constraints. To facilitate numerical calculations, the time-optimal velocity planning problem is discretized. Let N be the number of points of the discretized trajectory and the arc length of the ith point be written as s_i. The problem is discretized below:

$$\min_{\beta, \alpha \in \mathbb{R}^N} \quad \sum_{k=1}^{N} -\beta_k \tag{6}$$

subject to

$$\beta_{i+1} - \beta_i = 2\alpha_i(s_{i+1} - s_i), \tag{7}$$

$$v_{min,i}^2 \le \beta_i \le v_{max,i}^2, \tag{8}$$

$$\alpha_{min,i}^{\mathrm{L}} \le \alpha_i \le \alpha_{max,i}^{\mathrm{L}}, \tag{9}$$

$$\beta_i \le \frac{\alpha_{max,i}^N}{|\kappa(s)_i|}, \tag{10}$$

$$j_{min,i} \le \left(\frac{\alpha_{i+1} - \alpha_i}{s_{i+1} - s_i}\right)\sqrt{\beta_i} \le j_{max,i}, \tag{11}$$

$$T_{min,i} \le \sum_{k=1}^{i-1} \frac{s_{k+1} - s_k}{\sqrt{\beta_k}} \le T_{max,i}, \tag{12}$$

where $i = \{1, ..., N\}$. Velocity constraint is represented by (8), which is derived from four types of constraints: traffic rule, high precision map, comfort and dynamic constraints.

The longitudinal acceleration constraint is expressed in (9), while the ratio of lateral acceleration to curvature for velocity is described in (10). The Jerk constraint and obstacle avoidance constraint are defined in (11) and (12). However, due to the non-convex nature of (11) and the non-linear nature of (12), finding the optimal solution of problem (6) can be time-consuming, when the number of discretization points N is large.

To address this velocity planning problem, the present paper proposes a dynamic constrained frame strategy by using velocity filtering with acceleration as the threshold and applies the LP method twice to calculate the velocity.

ICI Bucharest © Copyright 2012-2023. All rights reserved

3. Dynamic Constraint Framework Strategy

When a solution for obstacle avoidance cannot be found within the hard constraint range, a dynamic constraint framework is created by dynamically relaxing comfort constraints based on the safe braking distance of the vehicle. This creates a safe velocity profile that can adapt to different dynamic environments, thus enabling obstacle avoidance.

When driving on urban or high-speed roads with heavy traffic, velocity planning is often preferred over lane changing when an obstacle enters the trajectory of the ego-vehicle. However, in dynamic environment, the hard constraint restriction may cause the velocity planner to fail in finding a safe obstacle avoidance solution. To overcome this limitation, the hard constraint dynamic relaxation algorithm is used to dynamically adjust the range of constraint frames.

The entire braking process is divided into a brake preparation phase, a brake starting phase and a full braking phase. Firstly, the braking preparation phase is the duration t_1 between the braking command and the braking operation, also known as the braking delay time. This section considers the time required for the vehicle to maintain its initial velocity at a constant rate, which is also the average time for the velocity planner to carry out a planning exercise. Secondly, during the brake starting phase, the vehicle decelerates at a rate of α_1. Limited by the maximum Jerk constraint from the current acceleration it was changed to α_1 after time t_2. The duration of this phase is t_2. Finally, in the full braking phase, the vehicle decelerates uniformly until it reaches the stationary obstacle (a parked car with a velocity of 0), which takes a duration of t_3.The vehicle safety braking distance D_1 represents:

$$D_1 = \begin{cases} v_{c0}t_c & t_c \le t_1 \\ v_{c0}t_1 + \int_{t_1}^{t_c} v_{c0}t\ dt - \int_{t_1}^{t_c} \frac{1}{2} j_{max}t^3\ dt & t_1 \le t_c \le t_2 \\ v_{c0}t_1 + \int_{t_1}^{t_2} v_{c0}t\ dt - \int_{t_1}^{t_2} \frac{1}{2} j_{max}t^3\ dt & \\ \quad + \frac{(\frac{1}{2} j_{max}t_2^2)^2 - v_{cf}^2}{2\alpha_1} & t_2 \le t_c \le t_3 \end{cases} . \quad (13)$$

where v_{co} and v_{cf} indicate the original planning speed of the ego-vehicle and the travel velocity of the obstacle vehicle, respectively.

It's important to note that the range of slack of the constraint frame is not infinite. For instance, the minimum braking deceleration is calculated as the safe braking distance of the vehicle at the initial moment of braking, using the distance S_1 from the vehicle on the path:

$$\alpha_{cmin}^{L} = \frac{(\frac{1}{2} j_{max}t_2^2)^2 - v_{cf}^2}{2\left[S_1 - v_{c0}t_1 - \int_{t_1}^{t_2} v_{c0}t\ dt + \int_{t_1}^{t_2} \frac{1}{2} j_{max}t^3\ dt) \right]} . \quad (14)$$

The road adhesion coefficient limits the maximum braking deceleration, and the maximum value is calculated by the formula:

$$\alpha_{min}^{L} = \mu g. \quad (15)$$

The road adhesion coefficient and the maximum vehicle deceleration are expresses as μ and μg, respectively. The dynamic range of the constraint frame can be obtained from (14) and (15). The range of the maximum safe acceleration of the vehicle is calculated using the lateral and longitudinal acceleration constraints and the road surface adhesion coefficients. The dynamic constraint frame of the vehicle is depicted in Figure 3, where the solution spaces of the normal friction circle, the constraint box, and the relaxation constraint are also shown.

The dynamic constraint frame offers greater maneuverability to ensure safe driving while maintaining as much comfort as possible. Ultimately, the algorithm dynamically adjusts the driving parameters of the ego-vehicle for different traffic conditions, allowing a successful velocity planning for obstacle avoidance.

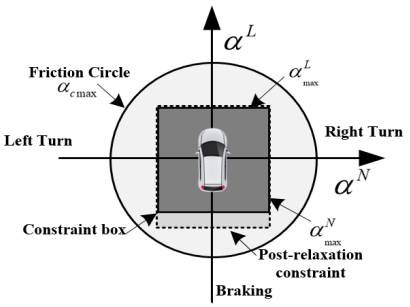

Figure 3. Schematic diagram of the vehicle dynamic restraint frame

4. Constraint Linearization Process

When Jerk and obstacle constraints are taken into account, velocity planning becomes a non-convex and non-linear problem. To address this issue, linear programming and obstacle velocity filtering

are combined in our method to the linearization of constraints, ensuring both high accuracy and computational efficiency. The linearization process encompasses three steps. Firstly, we devise a novel algorithm to filter obstacle velocities based on the acceleration threshold. This filtering converts the obstacle avoidance constraint into a maximum velocity constraint and completes the linearization process of the obstacle avoidance constraint. In the second step, the objective and constraints are used to perform the first linear programming, and an approximate velocity profile is obtained. This profile is then used to calculate the Jerk constraint, which is also linearized. Finally, in the third step, the linearized Jerk constraint is incorporated and a second linear programming is performed to generate the time-optimal velocity profile.

4.1 Obstacle Velocity Limiting Filtering

Instead of using obstacle avoidance constraint expressed in (12), acceleration is introduced as a filtering threshold, and a new approach of ego-vehicle obstacle avoidance is implemented by modifying the maximum velocity constraint. In this study, it is assumed that the trajectory of a dynamic obstacle follows a continuous linear function of its velocity, as demonstrated in (16).

$$s_{out}(t) = v_{obs}(t - t_{in}) + s_{in}, \quad t \in [t_{in}, t_{out}], \tag{16}$$

where s_{in} and s_{out} represent the arc lengths of the obstacle cut-in and cut-out on current path respectively, while t_{in} and t_{out} represent the obstacle cut-in and cut-out times respectively.

Define two deceleration thresholds α_A, α_B, subject to $\alpha_A \le \alpha_B$, and bring α_A, α_B in (13) to find the corresponding safety threshold distances D_A and D_B. Figure 4 illustrates a schematic example where the motion path of dynamic obstacles is indicated by the red dotted line, and the trajectory of the ego-vehicle with obstacle constraints is depicted by the green solid line.

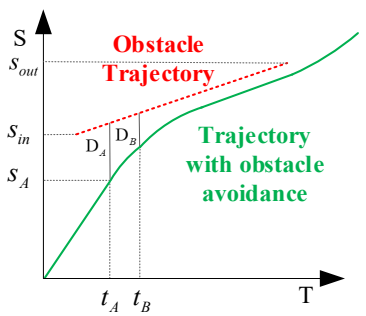

Figure 4. Schematic of the obstacle velocity limiting filtering algorithm

The ego-vehicle maintains its velocity at the original maximum velocity until it reaches a distance of D_A from the dynamic obstacle. When the distance to the obstacle is less than D_A, the maximum velocity is uniformly decelerated at S_A with a deceleration α_A. The current discrete point is defined as k and k+1 as next discrete point. The velocity during the pre-deceleration of the vehicle is adjusted as follows:

$$v_{k+1} = \sqrt{v_k^2 - 2\alpha_A(s_{k+1} - s_k)}. \tag{17}$$

When the distance between ego-vehicle and obstacle is less than D_B, the ego-vehicle decelerates uniformly at a deceleration α_B. The velocity of ego-vehicle is adjusted below:

$$v_{k+1} = \sqrt{v_k^2 - 2\alpha_B(s_{k+1} - s_k)}. \tag{18}$$

When the distance between the ego-vehicle and the obstacle is less than D_B, the ego-vehicle reduces its velocity to match that of the obstacle. Then, it follows the obstacle at the same velocity until it is no longer in the path of the ego-vehicle. Algorithm 1 provides further details of this process:

Algorithm 1. Obstacle Velocity Limit Filtering

Input: Obstacle Trajectory(s_{in}, t_{in}, t_{out})
Maximum Velocity Profile (s_{ego}, v_{max})
Output: Updated Maximum Velocity $\hat{v}_{max}$
for k = 1 to N -1 do
  Find (s_{obs}, t_{obs})which is nearest of (s_k,(s_{k+1} - s_k) / v_k);
  ds = $|s_k - s_{obs}|$;
  if ds < D_A then
    $\hat{v}_{max,k} = \sqrt{(v_{max,k-1})^2 - 2\alpha_A(s_k - s_{k-1})}$;
  else if ds < D_B then
    $\hat{v}_{max,k} = \sqrt{(v_{max,k-1})^2 - 2\alpha_B(s_k - s_{k-1})}$;
  else
    $\hat{v}_{max,k} = v_{max,k}$;
  end
end
return $\hat{v}_{max}$

where v_{max} represents the initial maximum velocity constraint. The maximum velocity constraint for N discrete trajectory points can be expressed as $v_{max} := [v_{max,1}, ..., v_{max,N}]^T$. The driving distance of vehicle on the travel path is denoted by S_{ego} in this paper, which can be expressed as $s_{ego} := [s_1, ..., s_N]^T$, and $\hat{v}_{max}$ represents the velocity constraint output after the obstacle velocity limit filtering.

ICI Bucharest © Copyright 2012-2023. All rights reserved

4.2 Linearization of Jerk Constraint

This step is the Jerk constraint processing. The Jerk constraint in (19) is expressed as:

$$j_i = (\frac{\alpha_{i+1} - \alpha_i}{s_{i+1} - s_i})\sqrt{\beta_i} = (\frac{\alpha_{i+1} - \alpha_i}{s_{i+1} - s_i})v_i. \quad (19)$$

Analysis of the above equation shows that the bilinear term $(\frac{\alpha_{i+1} - \alpha_i}{s_{i+1} - s_i})v_i$ causes Jerk constraint to become a non-linear constraint. To linearize Jerk constraint, one of the linear terms v_i needs to be fixed. The basic idea of the current study is to roughly estimate an optimized velocity profile and replace v_i in the optimization process, so that Jerk constraint becomes linear. In (Zhang et al., 2018), a pseudo-Jerk approach is proposed. This method achieves linearization of Jerk constraint by omitting one of the linear terms v_i. This transformation results in the Jerk constraint being changed from the first-order derivative of acceleration with respect to time to the first-order derivative of acceleration with respect to arc length s. However, the Pseudo-Jerk value obtained through this method is lower than the actual Jerk value over a wider range of velocity. For instance, when the ego-vehicle is at high velocity, the Pseudo-Jerk value becomes infinite while the ego-vehicle velocity is 0 because the velocity term is omitted. This significant difference makes the Pseudo-Jerk value less reliable than the actual Jerk constraint value.

The maximum acceleration and Jerk constraint for Forward-backward Jerk filtering used in (Shimizu, Horibe & Watanabe, 2022) give an estimated maximum velocity profile v_p to fix v_i. This method is equivalent to amplifying the current velocity v_i, so in $j_{min,i} \le (\frac{a_{i+1} - a_i}{s_{i+1} - s_i})v_{p,i} \le j_{max,i}$ constraint, the actual range of the Jerk constraint is reduced, limiting the acceleration change and potentially leading to failure in obtaining a linear programming solution in critical Jerk cases.

Therefore, this paper presents a new linear programming approach based on the Jerk linearization method, building on studies in (Shimizu, Horibe & Watanabe, 2022; Zhang et al., 2018). By omitting the non-linear Jerk constraint, the first linear programming step aims to find a more accurate predicted velocity profile. The result of first linear programming is expressed as β_k^*, and the linearization of Jerk constraint is completed by replacing v_i in the bilinear term $(\frac{\alpha_{i+1} - \alpha_i}{s_{i+1} - s_i})v_i$ of Jerk constraint with the result β_k^* being he approximate optimal solution. The final velocity profile is obtained by applying the linearized Jerk constraint on this issue and implementing a second linear programming solution.

Under the constraints (7), (8), (9), (10), first linear programming method is used to solve function (6). The problem is convex and can be verified as such. For readers who are unfamiliar with convex optimization, please refer to (Boyd & Vandenberghe, 2004) for details. In short, it can be seen from (6) that the objective is a negative power function and hence convex. Due to the linearity of the derivative, β and α exhibit a convex relationship, making equation (7) convex. For the inequality constraints of velocity and acceleration, the constraints on β and α from the equation and inequality are linear, making them convex as per equations (8) and (9). In relation to the normal acceleration constraint $(\frac{\alpha_{\max,i}^N}{|\kappa(s)_i|})^2$, with curvature serving as the variable (essentially acting as a constant value), the constraint manifests as the squared function of the absolute value of the curvature. Consequently, it exhibits convexity as illustrated in equation (10). In this paper, since function (6) is convex, the equation constraint (7) is mapped to each of the others, and since the inequality constraints (8, 9, 10) are convex, the optimization problem is convex.

4.3 Second Linear Programming

After the obstacle velocity limit filtering and the linearization of Jerk constraint, the linearized Jerk constraint (21) obtained from the first linear programming method is brought into function (6). Under the constraint conditions of (7), (8), (9), (10), (21), function (6) is solved by a second linear programming.

$$j_{min,i} \le (\frac{\alpha_{i+1} - \alpha_i}{s_{i+1} - s_i})\sqrt{\beta_i^*} \le j_{max,i}. \quad (20)$$

This is a linear programming problem that can be solved efficiently. The time-optimal velocity v_i is finally obtained through the obstacle velocity limit filtering and linear programming method for two times, which is shown as:

$$v_i = \sqrt{\beta_i}. \quad (21)$$

β_i^* is the optimal solution of velocity obtained through the first linear programming and it ensures that the optimization result does not exceed the velocity and acceleration limits. The cost function of the optimization makes the velocity as large as possible. The velocity profile, after the initial linear programming solution, doesn't deviate much from the actual velocity. This approximation ensures a higher level of accuracy in maintaining the Jerk constraint. Compared with (Zhang et al., 2018) and (Shimizu, Horibe & Watanabe, 2022), this approach of approximate linearization of Jerk using the results of linear programming is more precisely.

5. Simulation Experiments

In this section, the proposed optimization-based time-optimal velocity planning method is tested using simulations, considering a variety of scenarios. The same numerical experiments as those in (Shimizu, Horibe & Watanabe, 2022) are chosen to perform challenging velocity planning numerical experiments under various scenarios. The velocity of the future 30m trajectory of the vehicle is solved by planning algorithm in the experiment. In addition, the sample size of path is set as N=300 and the distance of sampled path points is set as $ds = 0.1m$. The acceleration constraint and Jerk constraint are set as $\alpha_{max,i}^{L} = 2.0m/s^2$, $\alpha_{min,i}^{L} = -2.0m/s^2$, $\alpha_{max,i}^{N} = 0.6m/s^2$, $j_{max,i} = 1.0m/s^3$ and $j_{min,i} = -1.0m/s^3$. These constraints will be applied in several subsequent application scenarios.

5.1 Experimental Scenario of Traffic Participant Cutting into the Trajectory of the Ego Vehicle

In the first simulation scenario, the initial values of the ego-vehicle velocity, acceleration and Jerk constraint are $v_0 = 2.5m/s$, $\alpha_0 = 0.0m/s^2$, $j_0 = 0.0m/s^3$ respectively. Deceleration thresholds are set to $\alpha_A = 0.8m/s^2$, $\alpha_B = 1.5m/s^2$. Set the traffic participant parameters as follows: velocity is v_{obs} = 1.0m/s, cut-in time is $t_0 = 2.0s$, departure time is t_N = 8.0s, initial distance of the obstacle from the vehicle is S_0 =8.0m, and obstacle sizes are obs_{width} = 2.0m, obs_{length} = 4.0m, respectively.

5.1.1 Obstacle Velocity Limited Filtering

Firstly, the results of obstacle velocity-limited filtering are presented, as shown in the previous section. Figure 5 shows the filtered velocity profile for obstacle avoidance, where the blue solid line denotes the original displacement time relationship, the red dashed line denotes the mapping of obstacle travel in the S-T diagram, and the green solid line denotes the ego-vehicle maximum velocity constraint after applying the obstacle velocity limit filtering. The safety threshold distances $D_A = 3.31m$ and $D_B = 1.78m$ can be found according to the formula for the deceleration threshold in (13).

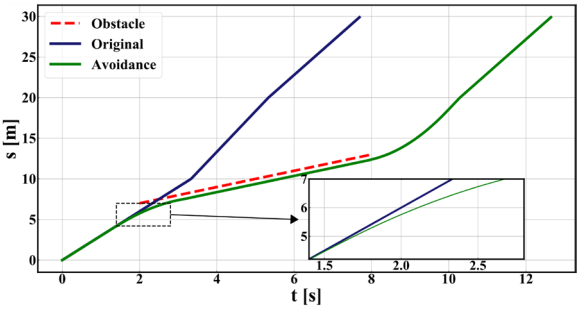

Figure 5. Obstacle vehicle velocity limitation filtered S-T diagram

The constraint track of the ego-vehicle (blue solid line) and the trajectory of the obstacle car (red dashed line) intersect (collide) at a distance of $s = 8.61m$ from the ego-vehicle and at $t = 2.87s$. By creating an obstacle velocity limitation filter profile, this algorithm completes the linearization of the obstacle avoidance constraint. As shown in obstacle velocity limiting filter profile (the green solid line), the distance between ego-vehicle and obstacle is less than D_A at $s = 3.6m$ and $t = 1.23s$. Then the vehicle runs into the first stage of deceleration and brakes with deceleration α_A, the distance between ego-vehicle and obstacle is less than D_B at $s = 4.8m$ and $t = 1.67s$. Next the vehicle runs into the second stage of deceleration and brakes with deceleration, the velocity of ego-vehicle is reduced to the same velocity as the obstacle vehicle until $s = 7.0m$ and $t = 2.90s$. The ego-vehicle performs an uniform velocity motion and maintains a distance of $0.91m$ until $t = 8.0$, when the obstacle leaves the path and ego-vehicle resumes the original velocity constraint.

The non-linear obstacle avoidance constraint can be transformed into a linear velocity profile constraint by employing this obstacle velocity limiting filter profile method, allowing the ego-vehicle to adjust accordingly.

ICI Bucharest © Copyright 2012-2023. All rights reserved

5.1.2 Initial Velocity Profile Generation

The initial velocity profiles meet the requirements of road velocity constraints, dynamic obstacle avoidance and other hard constraints. Figure 6 shows the distribution of the initial velocity profile of the ego-vehicle, where the red solid line indicates the original maximum velocity profile. By including the initial velocity profile into the Jerk constraint, the constraint can be linearized. The ink blue dashed line indicates the maximum velocity profile during dynamic obstacle avoidance. Moreover, the yellow solid line indicates the maximum velocity profile after the first LP filtering applied in this paper. The velocity profile obtained in this step provides the maximum velocity constraint for next linear programming step.

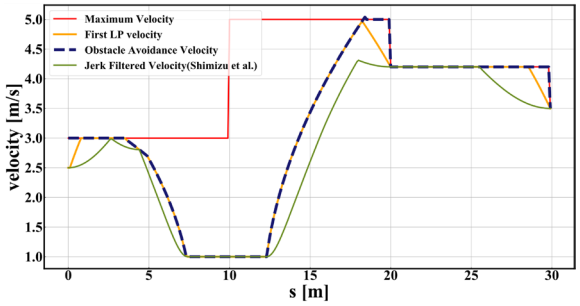

Figure 6. S-V diagram of the initial velocity profile

The method proposed in this paper is closer to the original Jerk constraint and alleviates the problem of solution space reduction caused by linearization. In conclusion, these results confirm that the proposed method can achieve maximum velocity constraint under comfort constraints.

5.1.3 Velocity Profile Solving

Figure 7 displays the velocity planning results of the algorithm proposed in this paper, in comparison with those of the algorithm proposed in (Shimizu, Horibe & Watanabe, 2022), at the same scenario. The diagram consists of three components: velocity, acceleration, and Jerk profile, with their values varying with distance *s*.

The purple dashed line represents the maximum velocity profile for dynamic obstacle avoidance. The green profile in the figure shows the final velocity profile obtained by using the obstacle velocity limiting filter with acceleration as the threshold and using LP twice, with a total trajectory time of 14.3 seconds. The red profile indicates the final velocity profile using the method from (Shimizu, Horibe & Watanabe, 2022), with a total trajectory time of 14.6 seconds. Additionally, compared with traditional filtering, this method may complete pre-acceleration preparation in $s = 11.8m$.

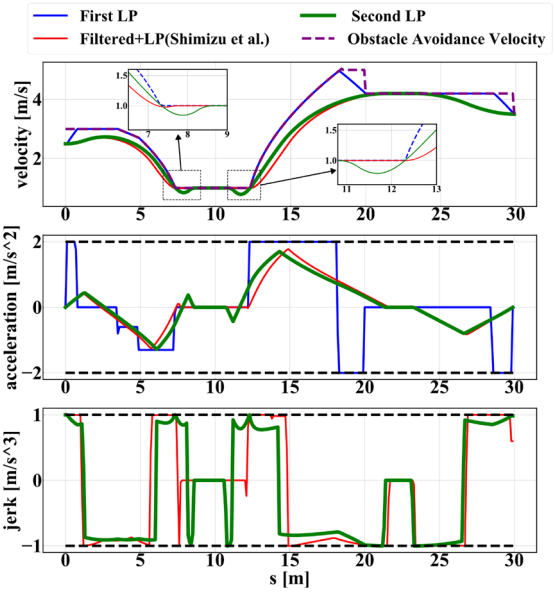

Figure 7. Velocity, acceleration and Jerk profile for the obstacle vehicle cut path scenario

Although the LP adopted for two times has the same velocity as the method proposed in (Shimizu, Horibe & Watanabe, 2022), when $s = 12.3m$, the LP adopted for two times has an acceleration of $1.31m/s^2$, when the ego-vehicle has better maneuverability, due to the pre-acceleration. Therefore, compared to this algorithm, the method proposed can better exploit the maneuverability of vehicle under the same constraints. In order to measure the comfort of velocity planning, it has been confirmed in (Mata-Carballeira, del Campo & Asua, 2021) that Jerk constraint plays a dominant role in influencing comfort. Therefore, the mean squared error of Jerk (JMSE) values is introduced as a criterion for evaluating comfort. The formula is as follows:

$$JMSE = \frac{1}{n}\sum_{i=1}^{n}(j_i - \hat{j}_i)^2 \tag{22}$$

The JMSE value obtained by means of the proposed method, as calculated using (22), is 0.64. In comparison, the JMSE value obtained by means of the Filtered-LP method applied in (Shimizu, Horibe & Watanabe, 2022) is 0.69. Therefore, the present velocity planning method yields a superior comfort metric for the generated velocity profiles compared to Filtered-LP method. In a word, the algorithm in this paper can find

the time-optimal velocity profile, acceleration profile and Jerk profile within a planned period of a dozen milliseconds, and all values are within the constraint range.

To better demonstrate the performance of the proposed method, experimental tests have been conducted on different vehicle speeds in the same scenario, as shown in Table 1.

The experimental comparison results show that the method is able to find an optimal solution that satisfies the constraints in various scenarios. In other words, the proposed method can generate a better solution to the original problem, without violating the original constraints.

5.2 Obstacle Start-stop Scenario Scene Avoidance Experiment

When a stationary object blocks the path of ego-vehicle or a red light is on, the test experiment scenario simulates the braking process to avoid obstructions. The purpose of experiment is to check whether the ego-vehicle can brake successfully to avoid obstacles at a safe distance from obstacles. Once the obstacles disappear from the track, it can resume motion planning.

In this scenario, the initial vehicle velocity value is $v_0 = 1.5m/s$. The remaining initial parameters remain unchanged. The traffic participant parameters are as follows: velocity is $v_{obs} = 0.0m/s$, cut-in time is $t_0 = 3.0s$, departure time is $t_N = 13.0s$, initial distance of the obstacle from the vehicle is $S_0 = 17.0m$.

In Figure 8, the representation of the line styles is made consistent with that in Figure 5. The constrained trajectory of ego-vehicle and the static obstacle trajectory are shown to intersect at a distance of $14.9m$ from the ego-vehicle, at $t = 4.13s$. Through the establishment of an obstacle velocity-limited filter profile, the linearization of the static obstacle constraint is accomplished. As depicted by the obstacle velocity-limited filter profile, the distance from the vehicle to the obstacle is observed to be less than $D_A = 5.65m$, when $s = 9.4m$ and $t = 3.13s$. At this point, the vehicle enters the first deceleration braking phase, applying a deceleration of $\alpha_A = 0.8m/s^2$, at $s = 12.1m$ and $t = 4.15s$, where the distance between the vehicle and obstacle is determined to be less than $D_B = 3.02m$. Subsequently, the vehicle is introduced into the second deceleration braking phase, with a deceleration of $\alpha_B = 1.5m/s^2$. Until $s = 14.2m$ and $t = 5.81s$, the velocity of the ego-vehicle is reduced to zero, allowing it to halt either before obstacles or at the red light stop line. This state is maintained until $t = 13.0s$, when the obstacle is observed to leave the path of the ego-vehicle or the commencement of the green light phase occurs, at which juncture the original velocity constraint of the vehicle is reinstated.

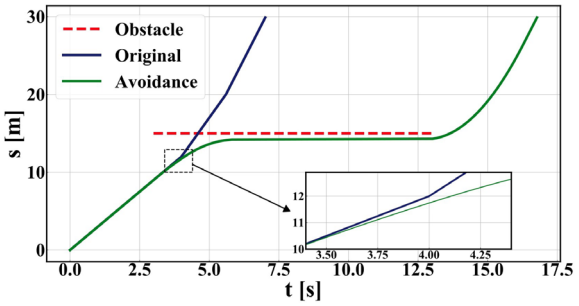

Figure 8. Obstacle velocity-limited filtered S-T diagram for the obstacle start-stop scenario

As it can be seen from the S-T diagram, the ego-vehicle can successfully complete obstacle avoidance by the restriction of obstacle velocity limiting filter profile. After linearization of obstacle constraint and Jerk constraint, it is possible to acquire the velocity, acceleration, and

Table 1. Comparison of experimental results for different vehicle velocities

Velocity of ego-vehicle (m/s)	Velocity of obstacle course (m/s)	Twice LP Total time taken(s)	Filtered-LP Total time (s) (Shimizu, Horibe & Watanabe, 2022)	Twice LP JMSN	Filtered-LP JMSN
2.0	1.0	14.4	14.6	0.58	0.67
2.0	1.5	13.3	13.6	0.62	0.68
2.0	2.0	12.1	12.4	0.61	0.66
2.5	1.0	14.3	14.6	0.64	0.69
2.5	1.5	13.0	13.4	0.63	0.69
2.5	2.0	12.0	12.2	0.59	0.64

ICI Bucharest © Copyright 2012-2023. All rights reserved

Jerk profile for obstacle scenario, as shown in Figure 9, by using LP twice.

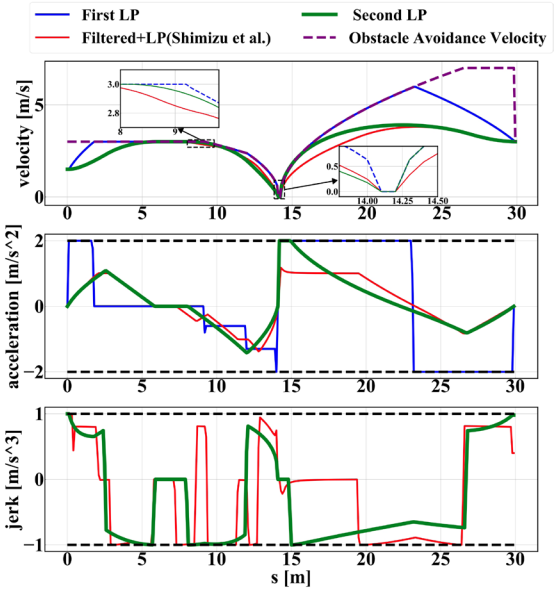

Figure 9. Velocity, acceleration and Jerk profile in obstacle start-stop scenario

The experiment results show that the total time taken for the trajectory planned to use twice LP is $12.9s$ and the total time taken for the trajectory using the method of (Shimizu, Horibe & Watanabe, 2022) is $13.3s$. Furthermore, in this scenario, the JMSE value obtained by the algorithm proposed in the present paper for velocity planning is 0.49, while the JMSE value obtained by the Filtered-LP method is 0.53.

The comparison reveals that the method proposed in this paper not only demonstrates lower total time consumption and improved timeliness in obstacle start-stop scene trajectories compared to the Filtered-LP method, but also offers superior comfort.

5.3 Dynamic Constraint Framework Strategy Experiments in Emergency Road Scenarios

One may encounter different emergency road scenarios while driving, such as when the ego-vehicle travels at high velocity and a traffic participant suddenly cuts in, or when a traffic participant ahead brakes urgently. In such cases, the planner may fail to solve the objective function under hard constraints and obtain an obstacle avoidance velocity profile. Therefore, to fully utilize the maneuverability of ego-vehicle and ensure its safety, it is necessary to relax the comfort constraints of problem.

In this scenario, the initial vehicle velocity value is $v_0 = 5.5m/s$. The remaining initial parameters remain unchanged. The traffic participant parameters are set as: velocity is $v_{obs} = 1.0m/s$, cut-in time is $t_0 = 1.0s$, departure time is $t_N = 8.0s$, initial distance of the obstacle from the vehicle is $S_0 = 15.0m$.

The hard constraint of traffic participants cutting into ego-vehicle trajectory scenario, in emergency scenarios, in maintained. In this scenario, the hard constraint approach used in (Shimizu, Horibe & Watanabe, 2022) causes the planner to fail in solving the objective function. However, the present dynamic constraint frame approach enables the generation of an obstacle avoidance velocity profile, through a relaxation strategy of hard constraint. The solution processes are shown in Figure 10.

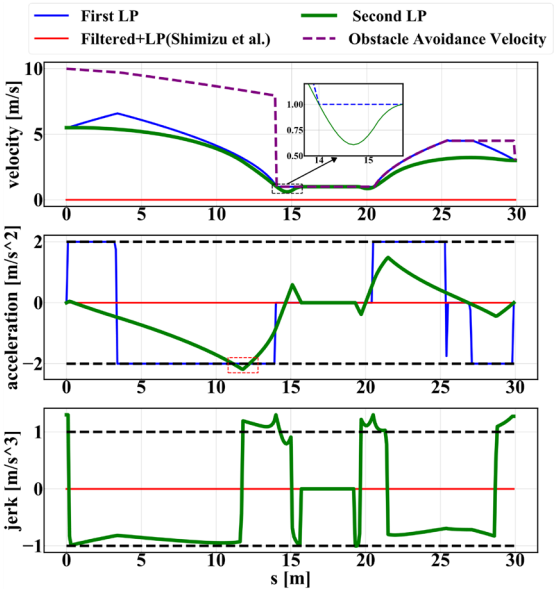

Figure 10. Velocity, acceleration and Jerk profile in emergency road scenarios

When velocity planner fails to solve the objective function under hard constraints, the hard constraint range of $\alpha^L_{min,i} = -2.0m/s^2$ can be extended by relaxing the constraints. Firstly, the safe braking distance equation of (21) yields the slack variable which is $\alpha^L_{min,i} = -2.2m/s^2$, and the Jerk constraint obtains $j_{max,i} = 1.3m/s^3$, through a fallback strategy. Then, it performs dynamic adjustment of the constraint frame.

In Figure 10, when $s = 11.2 - 12.4m$, all the accelerations exceed the hard constraint $\alpha^L_{min,i} = -2.0m/s^2$, achieving the effect of hard constraint relaxation, and the planning for

obstacle avoidance is completed with a total trajectory time of 12.76s.

Through experimental validation, it has been demonstrated that greater maneuverability is provided by the dynamic constraint frame, ensuring safe driving, while maintaining maximum comfort. The driving parameters of the ego-vehicle are dynamically adjusted by the algorithm, enabling successful velocity planning for obstacle avoidance.

5.4 Discussion of Experiments

In the aforementioned section, a series of numerical experiments are conducted to examine the influence of different planning methods on velocity planning outcomes across multiple scenarios. The acceleration-based velocity filtering is employed and LP method is utilized twice, to solve the velocity planning problem. The experimental data showcases that the present method achieves lower overall time consumption and superior comfort metric. Furthermore, the adoption of a dynamic constraint framework enhances the robustness of the velocity planning process.

6. Conclusion

This paper describes a method for autonomous driving that computes time-optimal velocity profiles for given paths while satisfying velocity, acceleration, and Jerk constraints. The proposed method ensures a smooth velocity profile that provides a reference for the velocity controller and a comfortable ride experience for passengers. Furthermore, a series of numerical experiments demonstrate that the approach proposed in this paper outperforms existing velocity planners in terms of computational efficiency, accuracy, and safety. However, it is important to note that the current research has not considered energy consumption constraints. Future work will focus on addressing this limitation by developing an advanced algorithm that optimizes energy consumption while simultaneously providing the best possible trajectories. By incorporating energy efficiency considerations, a more comprehensive analysis of autonomous driving systems is envisaged.

Acknowledgements

The research reported in this work was supported by the Major Science and Technology Innovation Project No. 2020CXGC010110, from Shandong Province, by the Shandong Provincial Natural Science Foundation No. ZR2022MF345, by the Key Technology No. 2022-MS6-159 of the Ministry of Transport of the People's Republic of China, and by the Doctoral research start-up fund of Shandong Jiao Tong University No. BS2021015.

REFERENCES

Artuñedo, A., Villagra, J. & Godoy, J. (2021) Jerk-Limited Time-Optimal Speed Planning for Arbitrary Paths. *IEEE Transactions on Intelligent Transportation Systems*. 23(7), 8194-8208. doi: 10.1109/TITS.2021.3076813.

Boyd, S. & Vandenberghe, L. (2004) *Convex Optimization*. Cambridge, UK, Cambridge University Press.

Cabassi, F., Consolini, L. & Locatelli, M. (2018) Time-optimal velocity planning by a bound-tightening technique. *Computational Optimization and Applications*. 70(1), 61-90. doi: 10.1007/s10589-017-9978-6.

Chen, Z., Wu, S., Shen, S., Liu, Y., Guo, F. & Zhang, Y. (2019) Co-optimization of velocity planning and energy management for autonomous plug-in hybrid electric vehicles in urban driving scenarios. *Energy*. 263(1), 360-372. doi: 10.1016/j.energy.2022.126060.

Consolini, L., Locatelli, M. & Minari, A. (2022) A Sequential Algorithm for Jerk Limited Speed Planning. *IEEE Transactions on Automation Science and Engineering*. 19(4), 3192-3209. doi: 10.1109/TASE.2021.3111758.

Consolini, L., Locatelli, M., Minari, A. & Piazzi, A. (2017) An optimal complexity algorithm for minimum-time velocity planning. *Systems & Control Letters*. 103(1), 50-57. doi: 10.1016/j.sysconle.2017.02.001.

Fan, H., Zhu, F., Liu, C., Zhang, L., Zhuang, L., Li, D. Zhu, W., Hu, J., Li, H. & Kong, Q. (2018) Baidu Apollo EM Motion Planner. *arXiv* [Preprint] arXiv:1807.08048. [Accessed 1st April 2023].

Guarino Lo Bianco, C. (2013) Minimum-Jerk Velocity Planning for Mobile Robot Applications. *IEEE Transactions on Robotics*. 29(5), 1317-1326. doi: 10.1109/TRO.2013.2262744.

ICI Bucharest © Copyright 2012-2023. All rights reserved

Jian, Z., Chen, S., Zhang, S., Chen, Y. & Zheng, N. (2022) Multi-Model-Based Local Path Planning Methodology for Autonomous Driving: An Integrated Framework. *IEEE Transactions on Intelligent Transportation Systems*. 23(5), 4187-4200. doi: 10.1109/TITS.2020.3042603.

Jones, M. L. H., Le, V. C., Ebert, S. M., Sienko, K. H., Reed, M. P. & Sayer, J. R. (2019) Motion sickness in passenger vehicles during test track operations. *Ergonomics*. 62(10), 1357-1371. doi: 10.1080/00140139.2019. 1632938.

Iancu, D., T., Nan, M., Ghita, S. & Florea, A. (2022) Trajectory Prediction Using Video Generation in Autonomous Driving. *Studies in Informatics and Control*. 31(1), 37-48. doi: 10.24846/v31i1y202204.

Li, P., Pei, X., Chen, Z., Zhou, X. & Xu, J. (2022) Human-like motion planning of autonomous vehicle based on probabilistic trajectory prediction. *Applied Soft Computing*. 118(1), 1568-4946. doi: 10.1016/j.asoc.2022.108499.

Mata-Carballeira, Ó., del Campo, I. & Asua, E. (2021) An eco-driving approach for ride comfort improvement. *IET Intelligent Transport Systems*. 16(2), 186-205. doi: 10.1049/itr2.12137.

Ni, H., Ji, S., Liu, Y., Ye, Y. & Zhang, C. (2022) Velocity planning method for position-velocity-time control based on a modified S-shaped acceleration / deceleration algorithm. *International Journal of Advanced Robotic Systems*. 19(1), 42-59. doi: 10.1177/17298814211072418.

Perri, S., Guarino, L. & Locatelli, M. (2015) Jerk bounded velocity planner for the online management of autonomous vehicles. In: *Proceedings of the IEEE International Conference on Automation Science and Engineering, CASE 2015, 24-28 August 2015, Gothenburg, Sweden*. New Jersey, USA, IEEE Robotics & Automation Society. pp. 618-625.

Shimizu, Y., Horibe, T. & Watanabe, F. (2022) Jerk Constrained Velocity Planning for an Autonomous Vehicle: Linear Programming Approach. In: *Proceedings of the 2022 International Conference on Robotics and Automation, ICRA 2022, 23-27 May 2022, Philadelphia, PA, USA*. New Jersey, USA, IEEE Robotics & Automation Society. pp. 5814-5820.

Subotić, M., Softić, E., Radičević, V. & Bonić, A. (2022) Modeling of Operating Speeds as a Function of Longitudinal Gradient in Local Conditions on Two-Lane Roads. *Mechatronics and Intelligent Transportation Systems*. 1(1), 24-34. doi: 10.56578/mits010104.

Wang, M., Liu, Q. & Zheng, Y. (2021) A curvature-segmentation-based minimum time algorithm for autonomous vehicle velocity planning. *Information Sciences*. 565, 248-261. doi: 10.1016/j.ins.2021.02.037.

Yang, B., Song, X., Gao, Z. & Zhu, N. (2022) Trajectory planning for vehicle collision avoidance imitating driver behavior. In: *Proceedings of the Institution of Mechanical Engineers, Part D: Journal of Automobile Engineering*. 236(5). United Kingdom, SAGE Publications Inc. pp. 907-926. doi: 10.1177/09544070211030422.

Zhang, Y., Chen, H., Waslander, S. L., Yang, T., Zhang, S., Xiong, G. & Liu, K. (2018) Toward a More Complete, Flexible, and Safer Speed Planning for Autonomous Driving via Convex Optimization. *Sensors*. 18(7), 2185-2214. doi: 10.3390/s18072185.